Parahydrogen studies of H 2 addition to Ir(I) complexes containing chiral phosphine–thioether ligands: implications for catalysis

Raluca Malacea, Jean-Claude Daran, Simon B Duckett, John P Dunne, Cyril Godard, Eric Manoury, Rinaldo Poli, Adrian C Whitwood

Parahydrogen studies of H_2 addition to Ir(I) complexes containing chiral phosphine-thioether ligands: Implications for catalysis.

Raluca Malacea [a], Jean-Claude Daran [a], Simon B. Duckett*[b], John P. Dunne[b], Cyril Godard[b], Eric Manoury*[a], Rinaldo Poli[a] and Adrian C. Whitwood[b]

[a] *Laboratoire de Chimie de Coordination, CNRS, 205 Route de Narbonne, 31077 Toulouse Cedex, France*
[b]*Department of Chemistry, University of York, YO10 5DD, United Kingdom, sbd3@york.ac.uk*

Ir(CO)(CpFe(η^5-C_5H_3(PPh_2)CH_2SR)Cl [R = Ph and ^{t}Bu], containing a κ^2:*P,S* ligand, undergoes H_2 addition across the S-Ir-CO axis under kinetic control to form two distinct diastereoisomeric products, which then rearrange *via* S dissociation in a process that can be hijacked for useful catalysis, but ultimately form a single diastereoisomer of the thermodynamic product where the hydride ligands are *trans* to chloride and phosphine.

Introduction

The cyclopentadienyl group is one of the most common organometallic ligands and shows a wide range of coordination chemistry.[1] Functionalised cyclopentadienyl (Cp) based ligands containing phosphine donor groups form an increasingly important class of planar, prochiral multifunctional ligands. In the case of iridium, a novel dihydride complex that is capable of C-H activation with high diastereoselectivity has been prepared using this approach.[2] Expansion of this area into heterobimetallic systems featuring chiral ferrocenyl phosphines has however yielded dramatic contributions in both catalysis and organic synthesis.[3] In this case, the plane of symmetry between the cyclopentadienyl rings is broken to introduce chirality. The addition of further functional groups to the rings introduces lateral chirality (also know as planar chirality) into the ferrocene complex. Togni *et al.*,[4] Enders *et al.*,[5] and Carretero *et al.*[6] have prepared a number of novel ferrocenyl ligands containing both phosphine and sulfur donors and reported on their use in group 10 metal based catalysis. In many cases, such pendant donors are labile and catalytic activity can be enhanced by the presence of this stabilising influence.[7]

The examination of the oxidative addition of H_2 to d^8 square planar transition metal complexes has played a significant role in learning about bond activation reactions and hence appreciating the complexities of one of the important steps in hydrogenation and hydroformylation catalysis. The accepted mechanism of H_2 addition to square planar Ir(CO)Cl(PPh_3)$_2$ is concerted and occurs across the Cl–Ir–CO axis.[8] Recent work in our group has shown that a minor product is also formed by H_2 addition over the P–Ir–P axis (Scheme 1).[9] Studies by Crabtree *et al*. demonstrated that replacement of the Cl ligand of Vaska's complex by an alkyl group[10] enables the characterisation of a low temperature H_2 addition product where addition occurs across the P-Ir-P axis. In the case of IrPh(CO)(PMe_3)$_2$ the corresponding low temperature addition product has been shown to isomerise at 25°C to the *trans* phosphine containing isomer. Consequently, it can be deduced that when this reaction proceeds under kinetic control addition across the P-Ir-P axis results and that the thermodynamic product, corresponding to addition over the Ph-Ir-CO axis, is formed by subsequent isomerisation.

Scheme 1 here

Eisenberg *et al* showed that the analogue of Vaska's complex Ir(CO)(dppe)Br, containing a symmetrical bisphosphine (dppe = bis-diphenylphosphinoethane) adds H_2 over the more π-accepting P-Ir-CO axis to yield a kinetic product which subsequently isomerises to the corresponding thermodynamic arrangement where the hydride ligands are *trans* to bromide and phosphorus.[11] There is therefore a high level of complexity to what otherwise might be thought of as a simple reaction.

Sargent *et al* investigated the oxidative addition of H_2 to IrCl(CO)(dppe) by *ab initio* MO techniques[12] using two *cis* PH_3 groups to mimic the dppe ligand. They found that while addition over the P-Ir-Cl axis led to the formation of the more stable isomer, the lower energy transition state corresponded to addition across the P-Ir-CO axis. Similar model calculations for Vaska's complex[13] predicted that addition across the P-Ir-P axis proceeded *via* the more stable transition state for PH_3. However, upon changing to PMe_3, calculations revealed that the relative stabilities of the transition states were reversed. Sargent and Hall therefore predicted that complexes of the type IrCl(CO){P(OR)$_3$}$_2$ might give H_2 addition across the P-Ir-P axis due to the π- accepting ability of the phosphite ligand. However, when Crabtree and Hall *et al* tested this prediction [14] addition across the Cl-Ir-CO axis was still observed.

We now describe a new and high yielding route to Vaska's analogues containing ligands of the type PS and report on their reactivity towards hydrogen via studies that employ the parahydrogen (p–H_2) effect. The parahydrogen (p–H_2) effect has also been called PHIP (parahydrogen induced polarisation)[15] and PASADENA (parahydrogen and synthesis allow dramatically enhanced nuclear alignment).[16] This effect has been extensively reviewed.[17] Achievements in this that are relevant to this study include the demonstration by Aime *et al*. that $Os_3(\mu\text{-}H)_2(CO)_{10}$, a species with magnetically equivalent hydrides, can be enhanced,[18] and that the enhanced hydride signal arises via the involvement of an intermediate with inequivalent hydrides. Similar studies involving $Ru_3(CO)_{11}$(NCMe) yielded an enhanced emission signal for molecular hydrogen that indicated a reversible interaction of p–H_2 with the Ru_3 cluster containing inequivalent hydrides.[19] Remarkably, the PHIP approach has enabled the observation of an intermediate that contains an agostic hydride during hydrogenations with a chiral rhodium system.[20] More recently, PHIP has been employed in the sensitisation of a hydroformylation product containing a single p–H_2 atom[21] and the transfer of polarisation via a ^{13}C nucleus to deuterium after the

hydrogenation of a perdeuterated substrate.[22] This technique has also been used to enhance organic components that lie within a metal's ligand sphere during catalysis.[23]

Experimental section

General conditions and reagents.

All reactions and purifications were carried out under nitrogen using glove box, high vacuum or Schlenk line techniques. $[Ir(COD)Cl]_2$ was prepared according to standard methods.[24] The PS ligands (**2-Ph** and **2-^{t}Bu**) were synthesised from racemic 2-(diphenythiophopshinoferrocenyl) in methanol according to the literature.[25]

NMR experiments.

NMR measurements were made using NMR tubes fitted with J. Young valves and solvents were added by vacuum transfer on a high vacuum line. For the parahydrogen induced polarization (PHIP) experiments, hydrogen enriched in the *para* spin state was prepared by cooling H_2 to 20 K over a paramagnetic catalyst (Fe_2O_3 doped silica) as described previously.[26] All NMR studies were carried out with sample concentrations of approximately 1 mM and spectra were recorded on a Bruker DRX–400 spectrometer with ^{1}H at 400.13, ^{31}P at 161.9, ^{13}C at 100.0 and ^{15}N at 40.5 MHz respectively. ^{1}H NMR chemical shifts are reported in ppm relative to residual ^{1}H signals (toluene–d_7, δ 2.13, $CHDCl_2$, δ 5.29, benzene-d_5, δ 7.13), ^{31}P NMR in ppm downfield of an external 85% solution of phosphoric acid, ^{13}C NMR relative to toluene–d_8, δ 21.3 and CD_2Cl_2, δ 21.6. Modified COSY, HMQC and nOe sequences were used as described.[27]

Synthesis of Ir(CO)(PPh_2FcCH_2SPh)(Cl) (1-Ph)

240 mg (0.488 mmol) of (R/S)-2-diphenylphosphino-(phenyl-thiomethyl)ferrocene (**2-Ph**) was dissolved in dichloromethane (4 mL) in a Schlenk tube and 163 mg (0.244 mmol) of $[Ir(COD)Cl]_2$ added under nitrogen. The solution was stirred for 10 minutes at room temperature and then 10 mL of hexane added. The yellow precipitate was dissolved in toluene (4mL) and 15 mL of hexane added. The solution was then purged with CO for 2h, concentrated in vacuo and a new yellow precipitate collected. The solid was washed with hexane. 294 mg of **1-Ph** was obtained (yield 81%). Crystals of the product were obtained by the slow diffusion of pentane into a dichloromethane solution. Microanalysis: Found C 45.46 %, H 3.75 %, Calculated C 45.47 %, H 3.28 % for a sample containing 0.75 moles CH_2Cl_2, as confirmed by NMR spectroscopy. IR: ν_{CO}: 1989 cm^{-1}, CH_2Cl_2. NMR data for **1-Ph** is presented in table 1.

Synthesis of Ir(CO)($PPh_2FcCH_2S^tBu$)(Cl) (1-^{t}Bu)

272 mg (0.576 mmol) of (R/S)-2-diphenylphosphino-(t-butyl-thiomethyl)ferrocene (**2-^{t}Bu**) was dissolved in dichloromethane in a Schlenk tube (3mL) and 193 mg (0.288 mmol) of $[Ir(COD)Cl]_2$ added under nitrogen. The solution was stirred for 2h at room temperature and then 10 mL of hexane added. The yellow precipitate obtained was dissolved in dichloromethane (5mL), and 15 mL of hexane added. The solution was then purged with CO for 2h, and concentrated in vacuo to give a yellow precipitate. The solid was washed with hexane and 348 mg of (**1-^{t}Bu**) (R/S)-2-diphenylphosphino-(t-butylthiomethyl)ferrocene-Ir(Cl)(CO) obtained (yield 83%). Crystals of the product were obtained by the slow diffusion of pentane in a dichloromethane solution. Microanalysis: Found C 40.24 %, H 3.03 %, Calculated C 40.2 %, H 3.85 %.for a sample containing 1.5 moles CH_2Cl_2, as confirmed by NMR spectrsocpy. IR: ν_{CO}: 1983 cm^{-1}, CH_2Cl_2. NMR data for **1-^{t}Bu** is presented in table 1.

Table 1 here

Results

Synthesis and structures of Ir(CO)(PS)Cl complexes

The complexes Ir(CO)(PS)Cl **1-Ph** and **1-^{t}Bu** [PS = ($CpFe(\eta^5\text{-}C_5H_3(PPh_2)CH_2S(R)$; R = Ph, ^{t}Bu)] were prepared in high yield, by the addition of 2 equivalents of the appropriate PS ligand **2-R** (R= Ph, ^{t}Bu) to a CH_2Cl_2/hexane solution of $[Ir(COD)Cl]_2$ under an inert atmosphere, followed by the addition of CO.[28]

The carbonyl stretch for **1-Ph** (1989 cm^{-1}) is slightly shifted relative to that of **1-^{t}Bu** (1983 cm^{-1}) in agreement with the expected enhanced basicity of the S^{t}Bu vs. SPh group. The ^{31}P NMR spectra of **1-Ph** display a single resonance at δ 5.29, while for **1-^{t}Bu** the corresponding resonance was detected at δ 6.5. This trend is mirrored in the ^{13}C resonances for the CO ligand, with **1-Ph** having a chemical shift at δ 166.5, while **1- ^{t}Bu** is at δ 174.4. NMR data for these two species is presented in Table 1; nOe methods were used to assign the group orientations indicated in the in-set structural representation**.**

Crystals of **1-Ph** and **1-^{t}Bu** were obtained by slow diffusion of hexane into a dichloromethane solution. The X-ray structure of both complexes reveals that the planar chirality of the substituted ferrocene ligand controls the stereochemistry at sulfur, indeed only one diastereoisomer is formed. However, as both space groups are centrosymmetric, the unit cell contains the RR and SS racemates (Table 2) and the sulfur substituent points away from the C_5H_5 moiety.[7] The coordination geometry of both these structures is slightly distorted from the ideal square planar arrangement, as indicated by the ligand-metal-ligand bond angles which deviate from the usual 90^o and 180^o (Table 3). The phosphine ligands lie *trans* to the chloride, a characteristic seen in related P-N complexes (Figure 1a and 1b).[29,30]

Figure 1 here

Table 2 here

Comparison of these structures reveals the Ir-P bond length is longer for **1-Ph** (2.2207(14) Å) than for **1-^{t}Bu** (2.2137(9) Å). The Ir-Cl bond is also longer in **1-Ph** (2.3809(14) Å) when compared to **1-^{t}Bu** (2.3690(9) Å). Interestingly, the Ir-CO bond length is shorter for **1-Ph** at 1.814(7) Å, compared to 1.830(17) Å for **1-^{t}Bu**. This is indicative of a greater degree in back bonding to CO in **1-^{t}Bu** as indicated by the IR data and hence a metal centre with higher electron density. This suggests that the interaction with the sulfur centre therefore dramatically influences the electron density available to the metal. The Ir-S bond, is shorter in **1-Ph** (2.3821(15) Å) than that of **1-^{t}Bu** (2.4018(9) Å) in accordance with the proposed greater interaction.

Table 3 here

The Ir-P bond lengths[31] are similar to those found in related complexes such as Ir(CO)((diphenylphosphino)-N,N-dimethyl-aniline)Cl, where the Ir-P distance is 2.197(2) Å. For, Ir(CO)(1-(2-pyridyl)-2-(diphenylphosphino)ethane)Cl the Ir-P distance is 2.221(1) Å. Again, the corresponding Ir-P bond, Ir-C and C≡O distances reflect changes in the electron donation properties of the ligands.

It is worth pointing out that in **1-Ph**, there is half a molecule of CH_2Cl_2 disordered around an inversion centre in the unit cell. The occurrence of this solvent molecule results in a disordered distribution over two positions of one of the phenyl group of the PPh_2 moiety.

Reactivity of Ir(CO)(PS)Cl with *p*-H_2

The addition of H_2 to the Ir(CO)(PS)Cl complexes could in principle lead to a variety of stereoisomers. The results that we have accumulated using ligands **2-Ph** and **2-^{t}Bu**, under kinetically and thermodynamically controlled conditions, lead to the global Scheme 2. The diastereomeric products **3a** and **3b** result from the H_2 oxidative addition across the S-Ir-CO axis, whereas product **4** (only one diastereomer is observed) originates from the slower addition over the P-Ir-Cl axis. Products **5a** and **5b** result from the kinetic products **3** by an intramolecular isomerization process. The collective evidence leading to this global scheme is described in the following sections.

Scheme 2 here

a) Reactivity of 1-Ph with *p*-H_2

When a sample of **1-Ph** was prepared in C_6D_6 and placed under 3 atm. of *p*-H_2, the resulting ^{1}H NMR spectrum at 295 K yielded four hydride signals that contained antiphase features in addition to in-phase splittings due to a single phosphorus coupling (Figure 2). This situation is typical of that found for PHIP enhanced hydride resonances.[17] According to the size of the associated J_{PH} couplings, these hydride signals all show couplings to one *cis* phosphine ligand. COSY confirmed that the resonances at δ -5.92 (J_{HH} = -5 Hz; J_{HP} = 20 Hz) and δ -14.09 (J_{HH} = -5 Hz; J_{HP} = 19 Hz) arose from one complex (**3a-Ph**), while those at δ -6.42 (J_{HH} = -4 Hz; J_{HP} 22 Hz) and δ -13.45 (J_{HH} = -4 Hz; J_{HP} = 20 Hz) arose from a second species (**3b-Ph**).

Figure 2 here

The detected H_2 additions products **3a-Ph** and **3b-Ph** therefore contain two inequivalent hydride ligands which are *cis* to a phosphine ligand. On the basis of the hydride resonance peak areas, it can be concluded that there is a 2.9-fold preference for the formation of **3b-Ph** over **3a-Ph** at 295 K if it is assumed that there are identical enhancement factors for each of these species.

In order to probe the ligand arrangements in these species further, a ^{13}CO labelled sample was examined. Now the hydride signals at δ -5.92 and δ -6.42 exhibited extra splittings of 45 Hz due to *trans* hydride-^{13}CO couplings. Given the bidentate nature of the PS ligand, it can be concluded that the remaining hydride ligands must be placed *trans* to sulfur. The chemical shifts of the associated hydride resonances are consistent with this deduction.[32]

In the ^{13}C NMR spectrum, carbonyl signals were detected at δ 176.4 for **3a-Ph** and at δ 177.8 for **3b-Ph** while the corresponding ^{31}P resonances appear at δ -2.15 and δ -6.85, respectively. NMR data for these species can be found in Table 4. The similarity in the NMR data for **3a-Ph** and **3b-Ph** suggests that they correspond to two diastereoisomeric products that are formed by H_2 addition over the two unique π-accepting OC-Ir-S axes outlined in Scheme 3.

Scheme 3 here
Table 4 here

nOe connections from the hydride ligand *trans* to CO in **3a-Ph** were observed to resonances at δ 8.08 (*ortho* phenyl proton of the PPh group) and δ 4.23 (the η^5-C_5H_5 ring) and confirm the structure shown in Scheme 3 for **3a-Ph**.

During the parahydrogen based NMR experiments, the size of the polarisation falls away as stable products are formed in this reaction. After 20 minutes the hydride resonances for **3a-Ph** appear with normal intensities while those for **3b-Ph** show limited enhancement; it was at this point that the nOe data were collected for **3a-Ph**, using a 90^o read pulse to quench the parahydrogen effect. At this stage in the reaction, a new pair of unpolarised hydride resonances are observed at δ -7.32 (J_{HH} = -6 Hz, J_{HP} = 143 Hz) and δ -16.50 (J_{HH} = -6 Hz, J_{HP} = 6 Hz) due to **4-Ph**. The characteristics of these resonances indicate that they arise from hydride ligands that are *trans* to phosphine and chloride, respectively. This ligand arrangement matches that found in the thermodynamic product observed for H_2 addition to Ir(CO)Br(dppe)[11] and other systems.[10] For complex **4-Ph**, nOe connections place the hydride ligand that is *trans* to PPh_2 (δ -7.32) close in space to an ortho phenyl proton of the thioether (δ 8.42). The hydride ligand that is *trans* to Cl (yielding the δ –16.50 resonance) shows interactions to an η^5-C_5H_5 ring (δ 3.94) and an *ortho* phosphine phenyl proton (δ 8.14).

These data support the geometry of **4-Ph** indicated in Scheme 4. We note that the other diastereoisomer was not observed. Under these conditions, when the *p*-H_2 effect was quenched with a 90^o read pulse, the ratio of **3a** : **3b : 4** proved to be 1 : 1.5 : 0.5.

This reaction is, however, further complicated by the fact that in the early stages of reaction, when the signals for **3-Ph** are still substantially enhanced, four new *p*-H_2 enhanced resonances briefly appear at δ -9.43 (J_{HH} = -3 Hz and J_{HP} = 17 Hz) and δ -10.52 (J_{HH} = -3 Hz and J_{HP} = 123 Hz) for species **5a-Ph**, and at δ -9.46 (J_{HH} = -3 Hz and J_{HP} = 16 Hz) and δ -10.52 (J_{HH} = -3 Hz and J_{HP} = 123 Hz) for species **5b-Ph.** These signals are hardly visible at 295 K, but **w**hen a sample is warmed to 323 K, the signals for **5a-Ph** and **5b-Ph** initially appear with around 1.5 % the intensity of those dues to **3a-Ph**. After a few minutes, however, their relative intensities increase until they are 63 % of the intensity of the **3a-Ph** signals, which are also polarised in these spectra at this temperature. While the ratio of **3a-Ph** to **3b-Ph** (based on their hydride resonance intensities) is 1: 2.6, and hence slightly lower than that found at 295 K, the ratio of **5a-Ph** to **5b-Ph** is 1.7:1. The similarity in the NMR signatures of these two materials suggests that they also correspond to diastereoisomeric products, but now the hydride ligands are *trans* to CO and phosphine, respectively. Scheme 4 illustrates the structures of **5a-Ph** and **5b-Ph**.

Scheme 4 here

It should be noted, however, that neither **5a-Ph** nor **5b-Ph** can be formed by the direct addition of H_2 to **1-Ph**. In the corresponding EXSY spectra, no evidence of the interconversion of **3-Ph** into either **5a-Ph** or **5b-Ph** is evident on the NMR timescale. However, the *p*-H_2 enhanced signals that are observed for **5a-Ph** and **5b-Ph** show substantial emission character (higher degree of peaks below the spectral-baseline) at elevated temperatures. This suggests that **5a-Ph** and **5b-Ph** are formed from a species with inequivalent hydride ligands in a reaction that retains the hydride ligands on the metal. Hence, it can be concluded that **5a-Ph** and **5b-Ph** most logically arise via dissociative or non dissociative ligand rearrangement from **3-Ph**. The dissociative route to their formation might involve the hemilability of the P,S ligand or loss of CO or phosphine. Alternatively, if the rearrangement is non dissociative it might occur via a tunnelling mechanism,[33,34,35] as originally described by Muetterties for complexes $Fe(H)_2L_4$ and $Ru(H)_2L_4$ (where L is a phosphorus ligand), or involve the related trigonal twist mechanism as described by Mann.[36]

In order to test for the nature of the rearrangement process, a sample of **1-Ph** containing 4-methyl-pyridine (4mpy) was prepared and exposed to *p*-H_2. When this system was studied by NMR spectroscopy at 295K, signals for **3a-Ph** and **3b-Ph** were still seen in the same ratio as without 4mpy, but those of **4-Ph**, **5a-Ph and 5b-Ph** were now absent. Four new hydride signals were seen at δ -4.27 and -16.95, and δ -4.29 and -16.83 that are assigned to the products **6a-Ph** and **6b-Ph** respectively. These hydride signals appear as anti-phase doublets of doublets (see table 4) and show additional J_{HC} couplings of 50 and 3 Hz respectively when ^{13}CO is employed. The hydride ligands of the new products are therefore *trans* to CO and chloride.

When this study was repeated with ^{15}N labelled pyridine, two analogous species were produced, with hydride signals at δ –4.32 (overlapping) and δ –16.85 and δ –16.94. None of these resonances showed the large 15 Hz splitting that would have been indicative of hydride trans to pyridine.[37] This supports the product geometries shown in Scheme 5 for **6a-Ph** and **6b-Ph** (data not attributed to specific isomers). Upon warming the sample to 313 K, **4-Ph**, **5a-Ph and 5b-Ph** are still absent and the ratio of the two diastereoisomers **6a-Ph** and **6b-Ph** proved to be 1.54 : 1. This ratio is approximately equal to the ratio of **5a-Ph** to **5b-Ph** produced without 4mpy.

Scheme 5 here

We observed that at the beginning of the reaction the ratio between **3a-Ph** and **3b-Ph** was 1: 2.9 and after 20 min a new product (**4**) was formed and the ratio of **3a-Ph** : **3b-Ph : 4-Ph** became 1:1.5:0.5. We monitored the variation in proportion of the hydride containing species in solution from the 20 minute point for a further 7 days, although only the first 24 hr period is shown in Figure 3. These data were simulated to determine the observed first order rate constants for the interconversion of the three species. The results are summarized in Figure 4 (left). These data confirm that there is a kinetic preference for the formation of **3b-Ph**, in the original reaction of **1-Ph** with H_2. When the rate constants for the reversible interconversion of **3a-Ph** and **3b-Ph** are compared, there is a clear thermodynamic preference for the formation of diastereoisomer **3a-Ph** (k_{eq} 44.1). It should also be noted that the observed rate constant for the formation of **4-Ph** from **3b-Ph** is 15.9 times higher than the corresponding reaction involving **3a-Ph**. After 6 days, the simulation predicts that the ratio of **3a-Ph** to **3b-Ph** to **4-Ph** is 9.5:0.3:90.2 when the actual value was 8:0:92.

Figure 3 here

Figure 4 here

In order to probe the mechanism of the interconversion further, a sample of **1-Ph** was placed under H_2 for 20 minutes. At this point, the ratio of **3a-Ph** to **3b-Ph** to **4-Ph** in solution was 1:1.45:0.8. The sample was then degassed and refilled with an atmosphere of D_2. In the subsequent NMR measurements we observed that the level of ^2H incorporation into the reaction products **3a**, **3b** and **4** increased, with signal intensities of the hydride resonances of the three species continually dropping until they became very hard to measure. After 185 minutes, however, the ratio between the three species was 34:0:66 in accordance with the great reactivity of **3b-Ph** and the greater stability of **4-Ph**. When the observed intensities of the hydride resonances for the three species were compared with those obtained under H_2, the apparent interconversion rates for **3a-Ph**, **3b-Ph** and **4-Ph** failed to match those seen under H_2. This suggests that isomer interchange proceeds via reversible H_2 loss.

b) Reactivity of 1-^{t}Bu with *p*-H_2

When the addition of H_2 to **1-^{t}Bu** was examined at 295 K, four hydride signals due to the analogous products **3a-^{t}Bu** and **3b-^{t}Bu** were observed (see table 4). The hydride resonances at δ -6.41 (J_{HH} = -5 Hz; J_{HP} = 20 Hz) and δ -14.30 (J_{HH} = -5 Hz; J_{HP} = 20 Hz) are due to **3a-^{t}Bu**, while those at δ -6.62 (J_{HH} = -7 Hz; J_{HP} = 23 Hz) and δ -13.70 (J_{HH} = -7 Hz; J_{HP} = 19 Hz) are due to **3b-^{t}Bu**. As before, the hydride ligands for **3a-^{t}Bu** and **3b-^{t}Bu** which yield high field resonances are *trans* to CO.

The ratio of the hydride signals for **3a-^{t}Bu** to **3b-^{t}Bu** at 295 K proved to be 1:1.56 which suggests that there is still a kinetic preference for the formation of **3b-^{t}Bu** but that it is slightly reduced when compared to the same process in **1-Ph**. nOe connections from the hydride ligand that is *trans* to CO in **3a-^{t}Bu** were observed to an η^5-C_5H_5 ring at δ 4.58. In contrast, the hydride ligand that is *trans* to CO in **3b-^{t}Bu,** which appears at δ -6.62, showed connections to phenyl ring protons at δ 8.13 and δ 7.52.

These data reveal that similar H_2 addition characteristics apply to those found with the SPh derivative. Only one diastereoisomer of a stable product, **4-^{t}Bu,** is again visible, with hydride ligands lying *trans* to phosphine and chloride. In this case, the hydride ligand which resonates at δ – 17.06, and is *trans* to chloride, shows nOe connections to signals at δ 8.18 (strong, an *ortho* proton of the phosphine), δ 3.72 (weak, a C_5H_3 ring proton resonance), and δ 1.52 (weak, the ^{t}Bu group). NOe connections from the hydride ligand which is *trans* to phosphine, and resonates at δ –7.85, are significant only to the ^{t}Bu group at δ 1.52. These data confirm that this product has the same geometry as **4-Ph** shown in Scheme 3. Interestingly, at 313 K, the hydride resonances for **4-^{t}Bu** exhibit the PHIP effect, thereby demonstrating that this species can be formed by direct H_2 addition to **1-^{t}Bu**; this contrasts with the situation for **4-Ph** whose hydride resonances are not enhanced even at 343 K. As in the case of **1-Ph** further *p*-H_2 enhanced resonances due to **5a-^{t}Bu** and **5b-^{t}Bu** which are directly analogous to **5a-Ph** and **5b-Ph** appear (table 4).

The addition of 4mpy to a sample of **1-^{t}Bu** and *p*-H_2 now quenched the observation of the hydride signals of **5a-^{t}Bu** and **5b-^{t}Bu** (295K and 315K), but in this case we see polarised signals for **3-^{t}Bu** and **4-^{t}Bu.** We therefore conclude that the addition of 4mpy suppresses the formation of **5a-^{t}Bu** and **5b-^{t}Bu** by trapping the intermediate formed via the dissociative route involving hemilability of the P,S ligand.

We again monitored the change in concentration of **3a-^{t}Bu**, **3b-^{t}Bu** and **4-^{t}Bu** over a 7 day period (Figure 5). These data were simulated to determine the observed rate constants (/hr) for isomer interconversion, which are summarized in Figure 4 (right). As in the case of the addition to **1-Ph,** there is a kinetic preference for the formation of **3b-^{t}Bu**, in the original reaction of **1-^{t}Bu** with H_2, but a thermodynamic preference for the formation of diastereoisomer **3a-^{t}Bu**.

Figure 5 here

Catalytic Hydrogenation of diphenylacetylene

When a sample containing **1-Ph** and *p*-H_2 was warmed with an excess of diphenylacetylene, weakly polarised signals for *cis*-stilbene, indicative of catalytic hydrogenation, were observed in the corresponding NMR spectra. PHIP enhanced hydride signals were now seen for **3a-Ph** and **3b-Ph** in the ratio 1 : 2.9 for an 1 hr, while the corresponding signals for **5a-Ph** and **5b-Ph** were much stronger than was the case without diphenylacetylene. In addition, non-polarised hydride signals due to **4-Ph** slowly begin to appear in these spectra.

This change in reactivity must be due to the presence of diphenylacetylene and confirms that H_2 addition to **1-Ph** leads to species that are able to act as hydrogenation catalysts. When a 90° read pulse is used again the quench the *p*-H_2 effect, thermally populated signals for **3a-Ph** and **3b-Ph** are also seen in these experiments which demonstrates that they also have a sufficiently long lifetime to allow their observation. Nonetheless, the fact that their hydride resonances remain enhanced whilst there is *p*-H_2 and substrate available reveals that **1-Ph** must be regenerated and that the rate of conversion to **4-Ph** must be retarded. These data further suggest that the observation of **5-Ph** is promoted by the presence of diphenylacetylene. This is consistent with the promotion of an increased rate of *p*-H_2 introduction into this species, which could be achieved if it were directly involved in the hydrogenation process.

When a sample containing **1-^{t}Bu** and *p*-H_2 was warmed with an excess of diphenylacetylene, polarised signals for *cis*-stilbene were stronger than those seen with **1-Ph**. This suggests that the apparent rate of hydrogenation is far greater for the ^{t}Bu containing substituted system. The addition of diphenylacetylene now suppressed the observation of the hydride signals for **5a-^{t}Bu** and **5b-^{t}Bu** even though polarised signals for **3a-^{t}Bu, 3b-^{t}Bu** and **4-^{t}Bu** were clearly visible in the associated spectra**.** The resonances for these H_2 addition products were also visible for many minutes and discrete populations of them again developed during the experiments.

The failure to see **5a-^{t}Bu** and **5b-^{t}Bu** under hydrogenation conditions for **1-^{t}Bu** is consistent with the proposed formation via S-R de-coordination since efficient trapping with diphenylacetylene would prevent its observation. The enhanced observation of **5-Ph** for the **1-Ph** system suggests that while the promotion of hydrogen cycling leads to a larger net enhancement for the hydride resonances of **5-Ph** the binding of **S-Ph** competes effectively with that of the alkyne. This result is consistent with the greater catalytic activity of the ^{t}Bu system, since the more sterically demanding S^{t}Bu donor competes even less effectively with the alkyne for the analogous coordination site. It is also important to note that neither **5-Ph** nor **5-^{t}Bu** correspond to stable products with long lifetime since they are only visible transiently via the PHIP effect.

In order to monitor the overall activity of these systems, and hence confirm their relative activity, a CH_2Cl_2 solution of **1-Ph** and diphenylacetylene (ratio 1:100) was placed under 30 atmospheres of H_2 in an autoclave at 295 K and allowed to react for 24 hrs. At this point only 1.8% of the alkyne was converted into cis (0.3%) and trans stilbene (1.5%). When an analogous test was performed on **1-^{t}Bu**, 2.5% of the alkyne was converted into cis (0.8%) and trans stilbene (1.7%) after 24 hrs. These results reveal that under the NMR conditions both **1-Ph** and **1-^{t}Bu** are poor hydrogenation catalysts, albeit **1-^{t}Bu** is the best.

Discussion

Isomerization processes

From the experimentally observed intensities of the PHIP enhanced hydride signals, the **3a**/**3b** ratio at 295 K was 1:2.9 for the Ph systems and 1:1.56 for the ^{t}Bu system. If these data correspond to the difference in rates of H_2 addition on either side of the square plane over the S-Ir-CO axis (Scheme 2), then it is possible to conclude that there is a greater preference when the H_2 ligand approaches the metal as far away from the bulk of the ferrocenyl arm as possible. The kinetic mixture of products **3a** and **3b** then evolves in three different ways (particularly evident for the Ph system), thus three different processes must occur on different timescales: (*i*) transformation of **3b** to **3a**; (*ii*) transformation to **4** and (*iii*) formation of **5a** and **5b**.

Both the interconversion between **3b** and **3a** (requiring formal metal inversion) and the irreversible transformation of **3b** to **4** have been shown to proceed via H_2 elimination by the $^2\mathbf{H_2}$ labelling study. The latter deduction is further supported by the fact that PHIP is observed in the hydride resonances of **4-^{t}Bu**. Both **4-^{t}Bu** and **4-Ph** are therefore produced by H_2 addition across the P-Ir-Cl axis of **1**. There appears to be a much higher activation barrier for H_2 addition over this axis, leading to a much greater stereoselectivity than was found in the step leading to **3a** and **3b**. The mechanism of these transformations is summarized in Scheme 6. The metal inversion is faster (in both directions) for the **Ph** than for the **^{t}Bu** system (e.g. 0.44 s^{-1} vs 0.31 s^{-1} from **3a** to **3b**). As a result, the equilibrium constant, [**3a**]/[**3b**], indicates that **3a-^{t}Bu** is more thermodynamically stable relative to **3b-^{t}Bu** (K = 66.2) than is the case for **3a-Ph** (K = 44.1) relative to **3b-Ph.**

Scheme 6 here

It is interesting to compare the mechanism of the isomerization from **3** to **4** with an analogous process involving the isoelectronic Ru(II) system $Ru(CO)_2(dppe)H_2$, that has been studied recently in our laboratories.[38] For the Ru complex, the hydride, P and carbonyl ligands undergo rapid exchange processes in an intramolecular fashion. A DFT study has identified the nature of the transition state as a 5-coordinate dihydrogen complex with a square pyramidal structure where the H_2 ligand occupies the axial position.[38] If the iridium system would undergo a similar mechanism for the transformation of **3** to **4**, the structure of the intermediate would be as shown in brackets in Scheme 6. It can be seen that this mechanism would involve stereospecificity.

The Ru(II) and Ir(III) systems are different in two respects: (*i*) the mechanism is intramolecular for Ru(II), intermolecular for Ir(III); (*ii*) the exchange process is much faster for the Ru(II) complex. The reason for the first difference can be traced to the much greater stability of the square planar coordination geometry for the Ir(I) reductive elimination product relative to the isoelectronic Ru(0) product. Compounds of type $Ru(CO)_2(PR_3)_2$ have been isolated only with very bulky phosphine ligands such as PMe^tBu_2 and exhibit a different structure from that of the isoelectronic square planar Rh(I) and Ir(I) complexes.[39] The reason for this difference have been

understood and lead the Ru(0) system to bind more strongly even weakly acidic ligands such as H_2. Thus, the reductive elimination of H_2 from the Ru(II) system leads to a low energy transition state with a bound H_2 ligand at low energy, whereas the same process from the Ir(III) system leads to the expulsion of H_2. The second difference is related to the greater Ir-H bond strength relative to the Ru-H bond strength, leading to a much greater energy loss, thus a higher barrier, for the H_2 reductive elimination process.

The observed rate constants for the formation of **4** from **3b** are about the same for the two systems. In contrast the rate constant for the conversion of **3a** to **4** is higher for the Ph system than for the ^{t}Bu system. The net effect of these rate constant changes agrees with the higher rearrangement and catalytic activity found for the ^{t}Bu system.

Products **5a** and **5b** cannot be formed by the direct addition of H_2 to **1**. The fact that the PHIP enhanced hydride signals seen for **5** have substantial emission character at higher temperatures suggests that they are formed from species with inequivalent hydride resonances. The observation of larger signals for **5**, when substantial amounts of **3** have been formed suggests that **3** corresponds to this species.

A possible pathway for the isomerization of **3** to **5** that immediately comes to mind is a Bailar twist of the H_2Cl triangular face. Although the presence of this pathway cannot be excluded, the alternative mechanism involving reversible dissociation of the S arm of the bidentate P,S ligand, shown in Scheme 6, is unambiguously proven by the trapping experiments with 4-methylpyridine. This may well be the only pathway leading from **3** to **5**. It requires that the phosphorus donor moves into the coordination position left vacant by the dissociation of the S arm in the square pyramidal 5-coordinate intermediate (path (*i*) in Scheme 6). This indeed leads to a stereospecific transformation (**3a** to **5a** and **3b** to **5b**). It is interesting to note that migration of the CO ligand into the vacant coordination site (path (*ii*) in Scheme 6) would provide an alternative pathway for the interconversion of **3a** and **3b**, whose presence in parallel to the reversible H_2 dissociation cannot be excluded.

Alkyne hydrogenation catalysis

The observation that diphenylacetylene is hydrogenated catalytically, and at the same time the apparent isomerization of **3** to **4** is suppressed, demonstrates the ability of complexes **3** to bind and activate the unsaturated substrate, most likely by dissociation of the S arm of the hemilabile P,S ligand. Sulfur dissociation is expected to be rather facile for the **3** isomers because of the *trans* effect of the hydride ligand. However, complexes **3a** and **3b** are still observed under conditions in which catalysis occurs. Under these conditions, the system clearly cycles through the iridium hydride species to return to **1** since PHIP can be observed while hydrogenation is evident.

Conclusions

Here we have demonstrated that *p*-H_2 enhanced NMR spectroscopy offers the opportunity to separate kinetic and thermodynamic effects in reactions where several diastereoisomeric products are formed (Scheme 2 and 6). In this case, the binding characteristics of the P-S ligand, $CpFe(\eta^5\text{-}C_5H_3(PPh_2)CH_2S(R)$, have been shown to allow the formation of Ir(P-S)(CO)Cl (**1-R**). This system proves to add H_2 under kinetic control to yield two diastereoisomers of **3** where the dominant form (**3b**) is selected via steric control of the addition pathway. Hemilability of the sulfur donor has been demonstrated and harnessed for catalytic activity, but ultimately this system forms **4** as the main H_2 addition product.

Acknowledgments

We are grateful to the EPSRC, the CNRS, and the European Union for funding under the HYDROCHEM network (contract HPRN-CT-2002-00176).

References

† **X-ray data for 1-^{t}Bu, and 1-Ph and NMR data for the reaction products as ESI: See http://www.rsc.org/suppdata/cc/b0/b000000a/.**

(a)

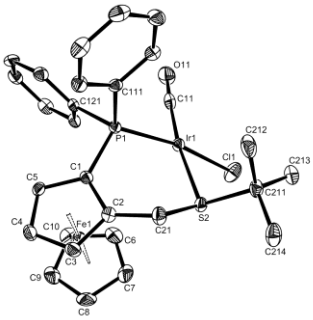

(b)

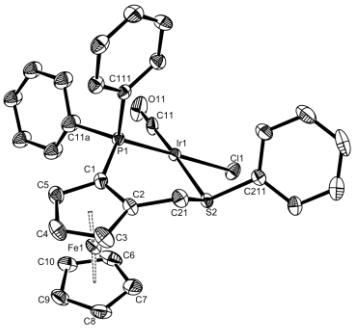

Fig. 1: (a) ORTEP diagram of Ir(CO)(PS)Cl **1-^{t}Bu**. (b) ORTEP diagram of Ir(CO)(PS)Cl **1-Ph**. Ellipsoids drawn at 50% probability level.

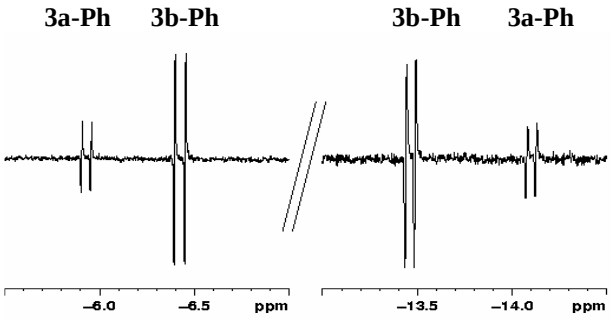

Fig. 2: Hydride region of a ^{1}H NMR spectrum recorded on a C_6D_6 solution of **1-Ph** reacting with *p*-H_2. Resonances for **3a-Ph** and **3b-Ph** are indicated.

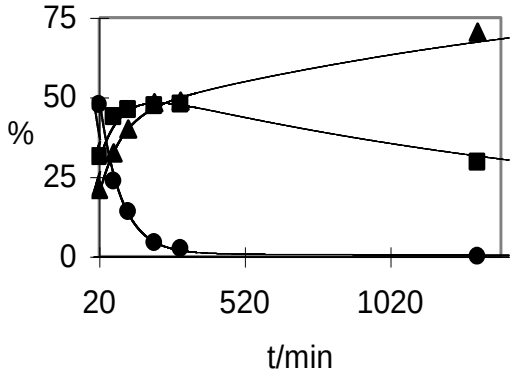

Fig. 3: Time profile for the conversion of **3a-Ph** (▪), **3b-Ph** (●) and **4-Ph** (▲) shown from 20 minutes to 18 hrs for a reaction at 295 K in C_6D_6.

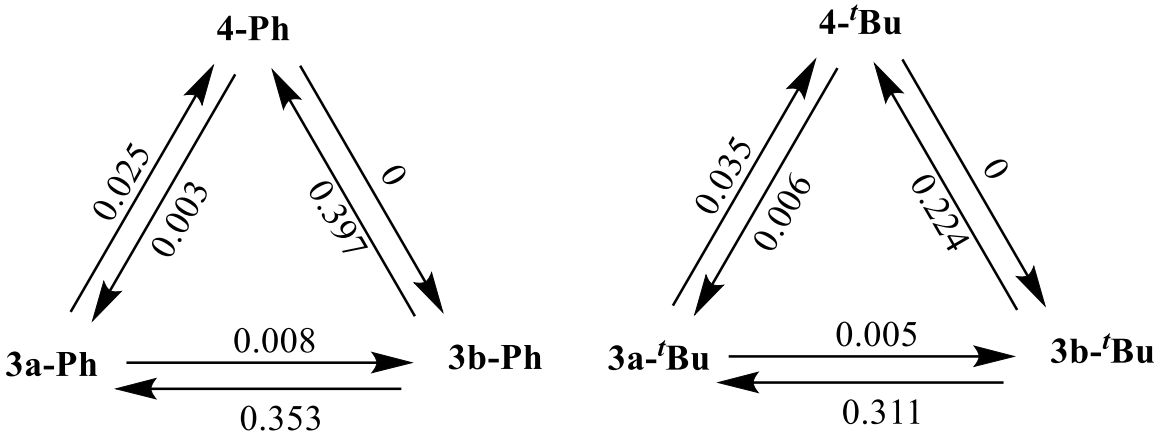

Fig. 4: Interconversion rate constants (h^{-1}) connecting **3a-R**, **3b-R** and **4-R**.

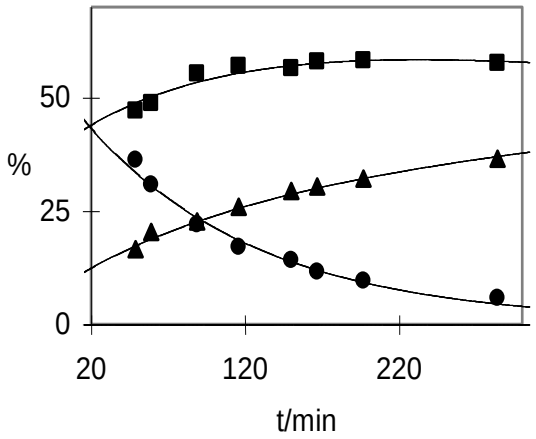

Fig. 5: Time profile for the conversion of **3a-^{t}Bu** (▪), **3b-^{t}Bu** (●) and **4-^{t}Bu** (▲) over 5 hrs for a reaction at 295 K in C_6D_6 .

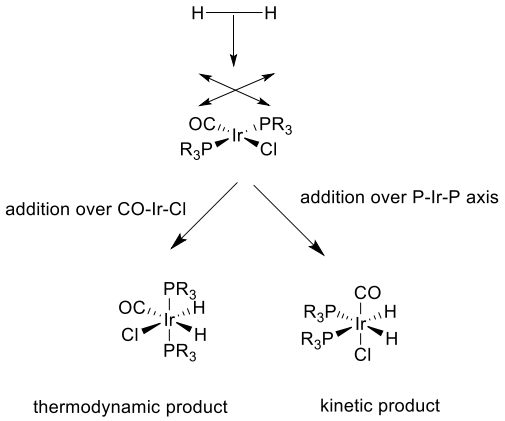

Scheme 1. Addition of H_2 to $IrCl(CO)(L)_2$ species

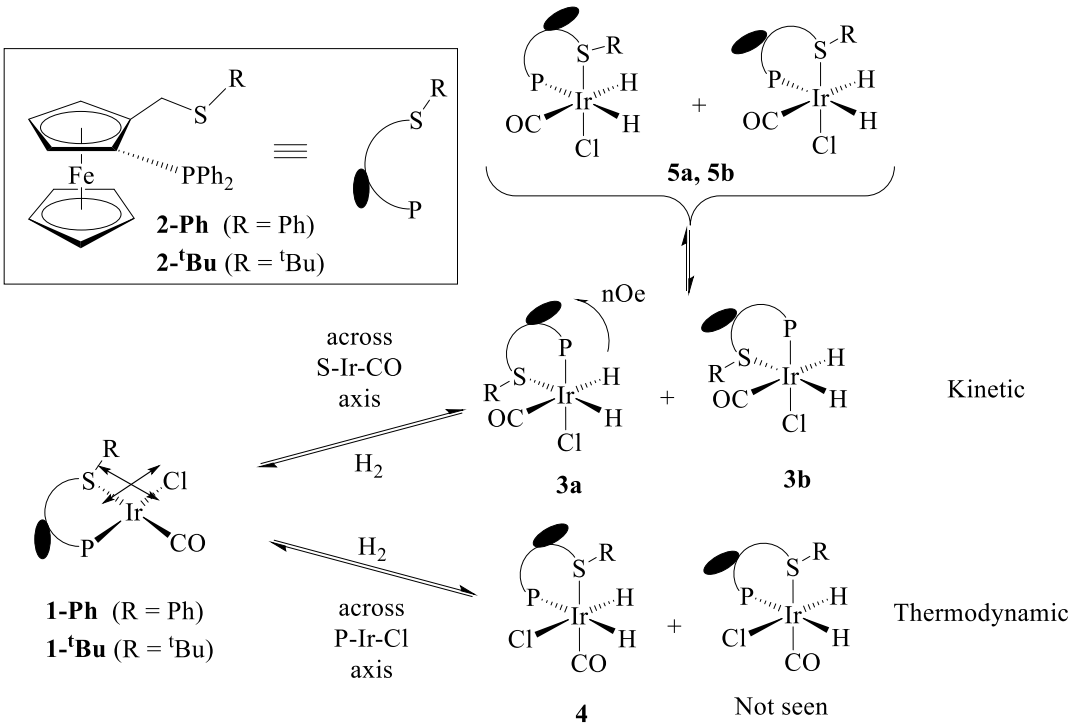

Scheme 2. H_2 addition to Ir(CO)((CpFe(η^5-C_5H_3(PPh_2)CH_2S(R))Cl, **1-R** (**R** = **Ph**, ***t*Bu**).

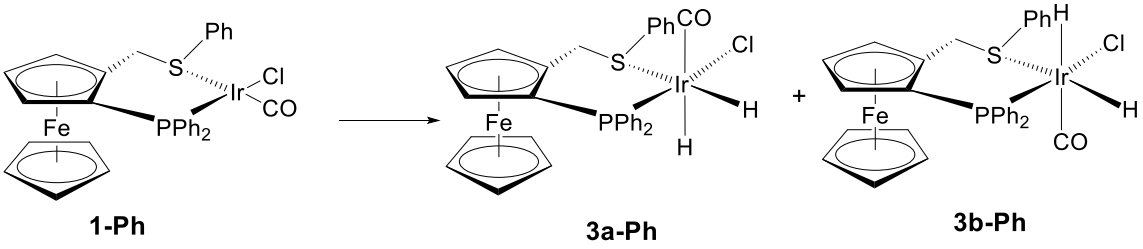

Scheme 3. H_2 addition to **1-Ph**.

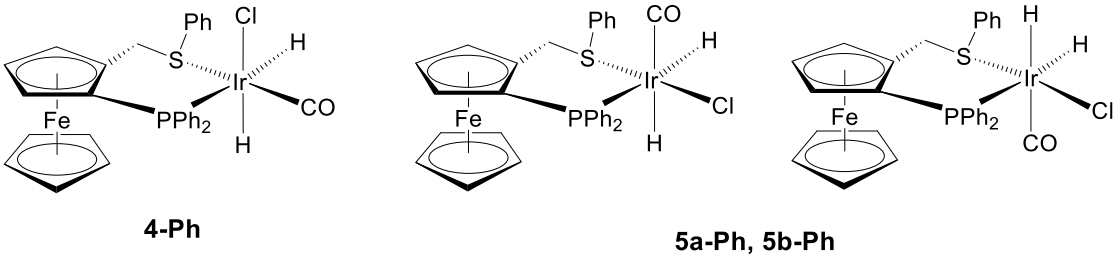

Scheme 4. Ligand arrangements for **4-Ph**, **5a-Ph** and **5b-Ph**.

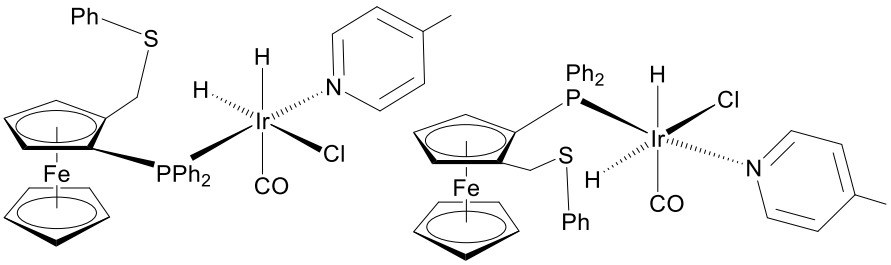

Scheme 5. Ligand arrangements for **6-Ph**.

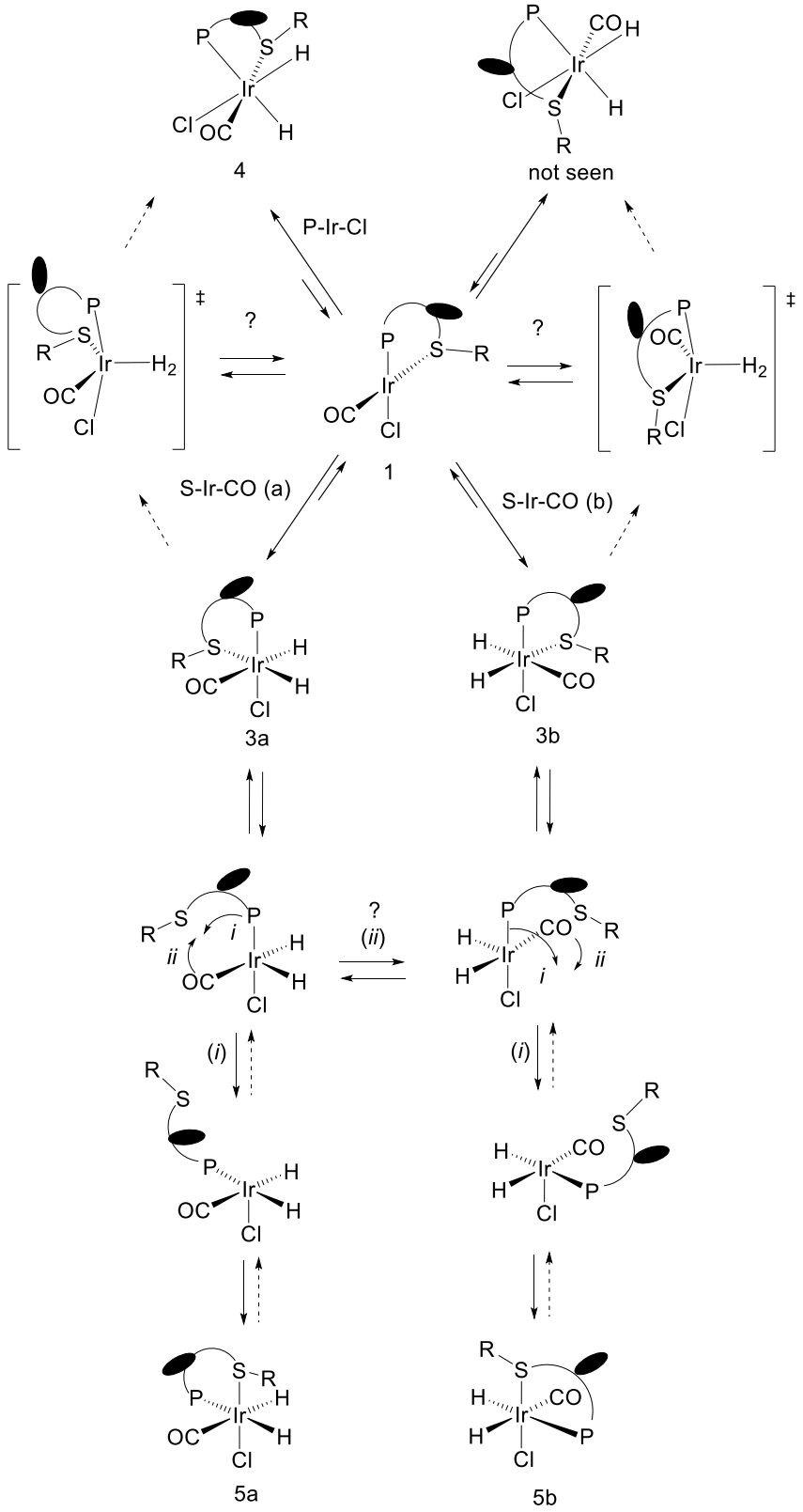

Scheme 6. Possible mechanistic pathways for the isomerization of complex **3**.

Table 1: NMR data for **1-^{t}Bu** and **1-Ph** in toluene-d_8

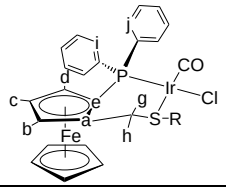

Nucleus, Assignment	Chemical shift (δ), coupling (Hz) **1-^{t}Bu**	Chemical shift (δ), coupling (Hz) **1-Ph**
^{1}H , P(*o*-Ph)i	7.78 (m)	7.72 (br)
P(*o*-Ph)j	7.58 (m)	7.60 (dd, 11 and 8)
P(*m*-Ph)i	7.13 (dd) J_{PH} = 2.2	6.98
P(*m*-Ph)j	7.09 (dd) J_{PH} = 2.3	6.97
P(*p*-Ph)i	7.12 (dd) J_{PH} = 2.2	6.99
P(*p*-Ph)j	7.08 (dd) J_{PH} = 2.3	6.96
Fc (η^5-C_5H_5)	4.65 (s)	4.41 (s)
Fc (η^5-C_5H_3) Hb	3.43 (d) J_{HH} = 2	3.83 (s)
Fc (η^5-C_5H_3) Hc	3.87 (t) J_{HH} = 2.2	3.73 (s)
Fc (η^5-C_5H_3) Hd	3.99 (d) J_{HH} = 2	3.40 (s)
CH_2-S , close to SR	2.94 (d) J_{HH} = 12	3.10 (d) J_{HH} = 15
CH_2-S, close to H_b	3.50 (d) J_{HH} = 12	3.44 (d) J_{HH} = 15
S-^{t}Bu	1.37 (s)	--
S-(*o*-Ph)	--	7.64
S-(*m*-Ph), S-(*p*-Ph) close to H_g	--	6.87
^{13}C , CO	174.4 (d) J_{PC} =14	166.5 (d) J_{PC} = 6
P(i-Ph) 1	130.5[a]	--
P(i-Ph) 2	130.0[a]	--
P(o-Ph)i	133.3[a]	133.9 (d) J_{PC} = 12
P(o-Ph)j	133.3[a]	133.3 (d) J_{PC} = 11
P(m-Ph)i	127.8[a]	128.4 (d) J_{PC} = 10
P(m-Ph)j	128.3[a]	128.3 (d) J_{PC} = 10
P(p-Ph)i	130.6[a]	130.7 (d) J_{PC} = 3
P(p-Ph)j	130.1[a]	130.2 (d) J_{PC} = 3
Fc (η^5-C_5H_5)	71.3	71.3 (overlap)
Fc (η^5-C_5H_3) C_a	67.3	71.3 (overlap)
Fc (η^5-C_5H_3) C_b	73.0	74.1 (d) J_{PC} = 8
Fc (η^5-C_5H_3) C_c	67.3	67.3 (d) J_{PC} = 7
Fc (η^5-C_5H_3) C_d	73.8	72.6 (d) J_{PC} = 4
Fc (η^5-C_5H_3) C_e	85.1	84.9 (d) J_{PC} = 17
CH_2-S	28.7	39.6
S-C(CH_3)	30.9	--
S-C(CH_3)	55.2	--
S-(*o*-Ph)	--	134.5
S-(*m*-Ph)	--	128.9
S-(*p*-Ph)		129.6
^{31}P, PPh_2	6.5	5.29

[a] obtained via low resolution HMQC measurement.

Table 2. Crystal data and structure refinement for **1–^{t}Bu** and **1-Ph**

complex	**1-^{t}Bu**	**1-Ph**
formula	$C_{28}H_{29}ClFeIrOPS$	$C_{30}H_{25}Cl$ FeIrOPS, $(CH_2Cl_2)_{1/4}$
M_r	728.04	768.76
T, K	115(2) K	180(2)
λ, Å	0.71073 Å	0.71073
Lattice	Monoclinic	Triclinic
Space group	P 2_1/c	P -1
a, Å	14.6773(11)	10.3886(11)
b, Å	8.0559(6)	10.4105(11)
c, Å	21.5594(17)	14.7920(14)
α, °	90.0	70.514(11)
β, °	95.933(2)	79.099(12)
γ, °	90.0	66.987(12)
Vol., Å3	2535.5(3)	1384.9(2)
Z	4	2
Dc, Mg/m^3	1.907	1.843
μ, mm^{-1}	6.087	5.624
F(000)	1424	748
size, mm^3	0.18 x 0.18 x 0.06	0.42 x 0.35 x 0.33
θ, range, °	1.39 to 25.03	2.13 to 26.04
Reflns coll.	19647	10375
unique reflns	4479 [R_{int} 0.0413]	5064 [R_{int} 0.0469]
Abs. cor.	Multi-scan	DIFABS
Max./min. transmission	1.000 / 0.697	0.8071 / 0.4243
Refinement	F^2	F^2
Data/restraints/ parameters	4479 / 0 / 310	5064 / 15 / 346
GOF on F^2	1.061	0.956
R indices [I>2σ(I)]	R1=0.0224, wR2=0.0540	R=0.0326, wR2=0.0673
R indices (all data)	R1=0.0258, wR2=0.0555	R= 0.0462, wR2=0.0709
$\Delta\rho_{max}$, $\Delta\rho_{min}$, e.$Å^{-3}$	1.592 , -0.381	1.242 , -1. 387

Table 3. Relevant bond lengths (Å) and angles (°) for **1–^{t}Bu** and **1-Ph**

	1–^{t}Bu	**1–Ph**
Ir(1)-Cl(1)	2.3690(9)	2.3809(14)
Ir(1)-C(1)	1.830(4)	1.814(7) Å
Ir(1)-P(1)	2.2137(9)	2.2207(14)
Ir(1)-S(2)	2.4018(9)	2.3821(15)
C(1)-O(1)	1.142(5)	1.157(8)
S(2)-Ir(1)-Cl(1)	85.64(3)	84.01(5)
S(2)-Ir(1)-C(11)	172.73(11)	174.5(2)
S(2)-Ir(1)-P(1)	95.08(3)	93.96(5)
C(11)-Ir(1)-Cl(1)	88.89(12)	92.8(2)

Table 4. NMR data for complexes **3** to **6**, in C_6D_6 at 295 K unless otherwise specified; see Schemes 2-5 for compound structures.

Compound	δ^1H	$\delta^{31}P\{^1H\}$	$\delta^{13}C\{^1H\}^a$
3a-Ph	-5.92, dd, J_{HH} = -5 Hz; J_{HP} = 20 Hz and J_{HC} = 45 Hz -14.09, dd, J_{HH} = -5 Hz; J_{HP} = 19 Hz and J_{HC} = 3 Hz	-2.15, s	176.4, d, J_{CP} = 3 Hz
3b-Ph	-6.42, dd, (J_{HH} = -4 Hz; J_{HP} 22 Hz and J_{HC} = 45 Hz -13.45, dd, J_{HH} = -4 Hz; J_{HP} = 20 Hz	-6.85, s	177.8, d, J_{CP} = 4 Hz
4-Ph	- 7.32 dd, J_{HH} = -6 Hz; J_{HP} = 143 Hz - 16.50 dd, J_{HH} = -6 Hz; J_{HP} = 6 Hz and J_{HC} = 5 Hz	-5.43, s	168.2, d, J_{CP} = 4 Hz
5a-Ph	- 9.43 dd, J_{HH} = -3 Hz; J_{HP} = 17 Hz and J_{HC} = 43 Hz - 10.52 dd, J_{HH} = -3 Hz; J_{HP} = 123 Hz and J_{HC} = 3 Hz	- 10.84, s	172.14, d, J_{CP} = 4 Hz
5b-Ph	- 9.46 dd, J_{HH} = -3 Hz; J_{HP} = 16 Hz and J_{HC} = 33 Hz - 10.52 dd, J_{HH} = -3 Hz; J_{HP} = 123 Hz and J_{HC} = 5 Hz	- 10.84, s	172.18, d, J_{CP} = 4 Hz
6a-Ph	- 4.27 dd, J_{HH} = -5 Hz; J_{HP} = 19 Hz and J_{HC} = 50 Hz - 16.95 dd, J_{HH} = -4 Hz; J_{HP} = 18 Hz and J_{HC} = 3 Hz	-2.6, s	178.5, d, J_{CP} = 5 Hz
6b-Ph	- 4.29 dd, J_{HH} = -5 Hz; J_{HP} = 19 Hz and J_{HC} = 50 Hz - 16.83 dd, J_{HH} = -5 Hz; J_{HP} = 19 Hz and J_{HC} = 3 Hz	-7.3, s	179.3, d, J_{CP} = 4 Hz
3a-^{t}Bu	-6.41, dd, J_{HH} = -5 Hz; J_{HP} = 20 Hz and J_{HC} = 52 Hz -14.30, dd, J_{HH} = -5 Hz; J_{HP} = 20 Hz	-2.6, s	176.6, d, J_{CP} < 4 Hz
3b-^{t}Bu	-6.62, dd, J_{HH} = -7 Hz; J_{HP} 23 Hz and J_{HC} = 54 Hz -13.70, dd, J_{HH} = -7 Hz; J_{HP} = 19 Hz	-6.7, s	178.15, d, J_{CP} < 4 Hz
4-^{t}Bu	- 7.85, dd, J_{HH} = -6 Hz; J_{HP} = 142 Hz and J_{HC} = 5 Hz - 17.06, dd, J_{HH} = -6 Hz; J_{HP} = 6 Hz and J_{HC} = 5 Hz	-7.86, s	168.7, d, J_{CP} = 4 Hz
5a-^{t}Bu	- 9.37, dd, J_{HH} = -3 Hz; J_{HP} = 15 Hz and J_{HC} = 40 Hz - 10.51, dd, J_{HH} = -3 Hz; J_{HP} = 122 Hz and J_{HC} = 5 Hz	-12.01, s	172.2, d, J_{CP} = 5 Hz
5b-^{t}Bu	- 9.40, dd, J_{HH} = -3 Hz; J_{HP} = 15 Hz and J_{HC} = 39 Hz - 10.51, dd, J_{HH} = -3 Hz; J_{HP} = 123 Hz and J_{HC} = 5 Hz	-12.01, s	172.6, d, J_{CP} = 4 Hz
6a-^{t}Bu	- 4.16, dd, J_{HH} = -4 Hz; J_{HP} = 18 Hz - 16.72, dd, J_{HH} = -4 Hz; J_{HP} = 19 Hz	-6.5, s	
6b-^{t}Bu	- 4.28, dd, J_{HH} = -4 Hz; J_{HP} = 19 Hz - 16.91, dd, J_{HH} = -4 Hz; J_{HP} = 18 Hz	-3.42, s	

a – ^{13}CO labelled sample (*ca.* 100% enriched);

Parahydrogen studies of H_2 addition to an Ir(I) complex containing a chiral phosphine- thioether ligand: Implications for catalysis.

Raluca Malacea[b], John P. Dunne,[a] Simon B. Duckett,[a] Cyril Godard,[a] Eric Manoury[b] and Rinaldo Poli[b]

[a] *Department of Chemistry, University of York, YO10 5DD, United Kingdom, sbd3@york.ac.uk*

[b] *Laboratoire de Chimie de Coordination, CNRS, 205 Route de Narbonne, 31077 Toulouse Cedex, France*

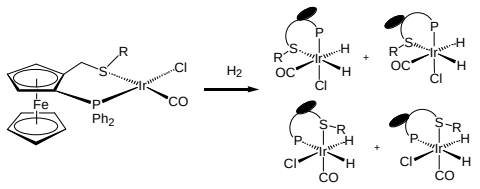

Ir(CO)(CpFe(η^5-C_5H_3(PPh_2)CH_2SR)Cl [R = Ph and ^{t}Bu], containing a κ^2:*P,S* ligand, undergoes H_2 addition across the S-Ir-CO axis under kinetic control to form two distinct diastereoisomeric products, which to ultimately form a single diastereoisomer of the thermodynamic addition product where addition occurs over the P-Ir-Cl axis.

1. H. Butenschon, Chem. Rev. 2000, 100, 1527-1564.
2. T. A. Mobley, R. G. Bergman. J. Am. Chem. Soc. **1998**, 120, 3253-3254.
3. T. J. Colacot. Chem. Rev. 2003, 103, 3101-3118.
4. J. Spencer, V. Gramlich, R. Hausel and A. Togni. Tetrahedron Asymmetry, 1996, 7, 41-44.
5. D. Enders. R. Peters, R. Lochtman and G.Raabe. Angew. Chem-Int. Ed. 1999, 38, 2421-2423. D. Enders, R. Peters, R. Lochtman, G. Raabe , J. Runsink and J. W. Bats. Eur. J. Org. Chem. 2000, 3399-3426.
6. O. G. Mancheno, J. Priego, S. Cabrera, R. G. Arrayas, T. Llamas and J. C. Carretero. J. Org. Chem. 2003, 68, 3679-3686. O. G. Mancheno, R. G. Arrayas and J. C. Carretero. Organomet. 2005, 24, 557-561.
7. K. Espinet and K. Soulantica, *Coord.Chem. Rev.*, 1999, **195,** 499. A. M. Masedeu-Bulto, M. Dieguez, E. Martin and M. Gomez. Coord. Chem. Rev. 2003, 242, 159-201.
8. L. Vaska, J. Di. Luzio, *J. Am. Chem. Soc*., 1961, **83,** 2784.
9. (a) S. K. Hasnip, S. B. Duckett, C. J. Sleigh, D. R. Taylor, G. K. Barlow and M. J. Taylor. *Chem. Commun.* 1999, 1717, (b) S. K. Hasnip, S. A. Colebrooke, C. J. Sleigh, S. B. Duckett, D. R. Taylor, G. K. Barlow and M. J. Taylor. *J. Chem. Soc. Dalton Trans,*. 2002, **4**, 743.
10. M. J. Burk, M. P. McGrath, R. Wheeler and R. H. Crabtree, *J. Am. Chem. Soc.*, 1988, **110**, 5034.
11. C. E. Johnson and R. Eisenberg, *J. Am. Chem. Soc.*, 1985, **107,** 3148.
12. A. L. Sargent, M. B. Hall and M. F. Guest, *J. Am. Chem. Soc.*, 1992, **114**, 517.
13. A. L. Sargent and M. B. Hall, *Inorg. Chem.*, 1992, **31**, 317.
14. X. Luo, D. Michos, R. H. Crabtree and M. B. Hall, *Inorg. Chim. Acta*, 1992, **200**, 429.
15 T. C. Eisenschmid, R. U. Kirss, P. A. Deutsch, S. I. Hommeltoft, R. Eisenberg, J. Bargon, R. G. Lawler and A. L. Balch, *J. Am. Chem. Soc.*, 1987, **109,** 8089.
16. C. R. Bowers and D. P. Weitekamp, *J. Am. Chem. Soc.*, 1987, **109**, 5541
17. (a) R. Eisenberg, *Acc. Chem. Res.*, 1991, **24,** 100. (b) J. Natherer and J. Bargon, *Prog. Nucl. Magn. Reson. Spectros.*, 1997, **31**, 293. (c) S. B. Duckett and C. J. Sleigh, *Prog. Nucl. Magn. Reson. Spectros.*, 1999, **34**, 71. (d) S. B. Duckett and D. Blazina, *Eur. J. Inorg. Chem.*, 2003, **16**, 2901. (e) D. Blazina, S. B. Duckett, J. P. Dunne and C. Godard, *Dalton Trans.*, 2004, **17,** 2601. (f) Recent Advances in Hydride Chemistry, Elsevier, ISBD: 0-4444-50733-7 Edit M Peruzzini and R Poli. 329-350.
18. S. Aime, R. Gobetto and D. Canet, *J. Am. Chem. Soc.*, 1998, **120**, 6770.
19. S. Aime, W. Dastru, R. Gobetto, A. Russo, A. Viale and D. Canet, *J. Phys. Chem. A.*, 1999, **103,** 9702.
20. R. Giernoth, H. Heinrich, N. J. Adams, R. J. Deeth, J. Bargon and J. M. Brown, *J. Am. Chem. Soc.*, 2000, **122,** 12381.
21. A. B. Permin and R. Eisenberg, J. Am. Chem. Soc., 2002, **124,** 12406.
22. S. Aime. R. Gobetto, F. Raineri and D. Canet, *J. Chem. Phys.*, 2003, **119,** 8890.
23. J. P. Dunne, S. Aiken, S. B. Duckett, D. Konya, K. Q. Almedia Lenero and E. Drent, *J. Am. Chem. Soc.*, 2004, 126, 16708-16709.
24. J. L. Herde, L. C. Lambert., C. V. Senoff. *Inorg. Synth*. 1974, **15**, 18.
25 L. Routaboul, S. Vincendeau, J.-C. Daran, E. Manoury, *Tetrahedron: Asymmetry* **2005**, *16*, 2685.
26 M. S. Anwar, D. Blazina, H. Carteret, S. B. Duckett, T. K. Halstead, J. A. Jones, C. M. Kozak and R. J. K. Taylor. *Phys. Rev. Lett.*.2004. **93**, 040501-040504.
27 (a) B. A. Messerle, C. J. Sleigh, M. G. Partridge, S. B. Duckett, *J. Chem. Soc. Dalton Trans.* **1999**, 1429. (b) S. A. Colebrooke, S. B. Duckett and J. A. B. Lohman, *Chem. Commun.* **2000**, 685. (c) P. Hubler and J. Bargon, *Angew. Chem. Int. Ed*. **2000**, *39*, 3701
28 M. J. Burk and R. H. Crabtree, *Inorg. Chem.*, **1986**, *25*, 931.
29 D. M. Roundhill, R. A. Bechtold and S. G. N. Roundhill, *Inorg. Chem.*, **1980**, *19*, 284.
30 M. P. Anderson, A. L. Casalnuovo, B. J. Johnson, B. M. Mattson, A. Mueting and L. H. Pignolet, *Inorg. Chem.*, **1988**, *27*, 1649.
31 M. R. Churchill and S. A. Bezman, *Inorg. Chem.*, **1974**, *13*, 1418.
32 (a) A. M. Mueting, P. D. Boyle, R. Wagner, L. H. Pignolet, *Inorg. Chem.*, **1988**, *27*, 271-279. (b) R. C. Linck, R. J. Pafford, T. B. Rauchfuss, *J. Am. Chem. Soc*. **2001**. *123*, 8856.
33 P. Meakin, E. L. Muetterties and J. P. Jesson, *J. Am. Chem. Soc.*, **1973**, *95*, 75.
34 P. Meakin, E. L. Muetterties, F. N. Tebbe and J. P. Jesson, J. Am. Chem. Soc., **1971**, 93, 4701.
35 J. P. Jesson, E. L. Muetterties and P. Meakin, J. Am. Chem. Soc., **1971**, 93, 5261.
36 G. E. Ball and B. E. Mann, *J. Chem. Soc., Chem. Commun.*, 1992, 561.
37 (a) B. T. Heaton, J. A. Iggo, C. Jacob, J. Nadarajah, M. A. Fontaine, R. Messere, A. F. Noels, *J. Chem Soc., Dalton Trans* 1994, 2875, (b) R Zhou, J. A. Aguilar, A. Charlton, S. B. Duckett, P. I. P. Elliott and R. Kandiah. *Dalton*, 2005, 3773.
38 D. Schott, P. Callaghan, J. Dunne, S. B. Duckett, C. Godard, J. M. Goicoechea, J. N. Harvey, J. P. Lowe, R. J. Mawby, G. Müller, R. N. Perutz, R. Poli, M. K. Whittlesey, *J. Chem. Soc., Dalton Trans.* **2004**, 3218-3224.
39 (a) M. Ogasawara, S. A. Macgregor, W. E. Streib, K. Folting, O. Eisenstein, K. G. Caulton, *J. Am. Chem. Soc.* **1995**, *117*, 8869-8870. (b) M. Ogasawara, S. A. Macgregor, W. E. Streib, K. Folting, O. Eisenstein, K. G. Caulton, *J. Am. Chem. Soc.* **1996**, *118*, 10189-10199.